

**( $^{16}\text{O}$ ,  $^{15}\text{N}$ ) and ( $^{12}\text{C}$ ,  $^{11}\text{B}$ ) reactions on  $^{54}\text{Fe}$  and  $^{62}\text{Ni}$  at  $E(^{16}\text{O}) = 104$  MeV  
and  $E(^{12}\text{C}) = 78$  MeV<sup>†</sup>**

F. D. Becchetti

*Cyclotron Laboratory, Physics Department, The University of Michigan, Ann Arbor, Michigan 48105  
and Lawrence Berkeley Laboratory, Berkeley, California 94720*

B. G. Harvey, D. Kovar,\* J. Mahoney, and M. S. Zisman<sup>‡</sup>

*Lawrence Berkeley Laboratory, Berkeley, California 94720*

(Received 27 June 1974)

The ( $^{12}\text{C}$ ,  $^{11}\text{B}$ ) and ( $^{16}\text{O}$ ,  $^{15}\text{N}$ ) reactions on targets of  $^{54}\text{Fe}$  and  $^{62}\text{Ni}$  have been studied at bombarding energies far above the Coulomb barrier:  $E(^{12}\text{C}) = 78$  MeV and  $E(^{16}\text{O}) = 104$  MeV, respectively. The reaction mechanism appears to be direct and is adequately described with the distorted-wave Born approximation, provided recoil effects are included. A comparison of heavy-ion and light-ion analyses permits  $j$  assignments to be made for some levels by utilizing the  $j$  dependence of the heavy-ion reactions.

[NUCLEAR REACTIONS  $^{54}\text{Fe}(^{16}\text{O}, ^{15}\text{N})$ ,  $^{62}\text{Ni}(^{16}\text{O}, ^{15}\text{N})$ ,  $E = 104$  MeV;  $^{54}\text{Fe}(^{12}\text{C}, ^{11}\text{B})$ ,  $^{62}\text{Ni}(^{12}\text{C}, ^{11}\text{B})$ ,  $E = 78$  MeV; measured  $\sigma(E_f, \theta)$ ; DWBA analysis;  $^{55}\text{Co}$  and  $^{63}\text{Cu}$  levels deduced  $j$  values and spectroscopic factors. Resolution 100–200 keV.]

## I. INTRODUCTION

This study of single nucleon transfers at energies well above the Coulomb barrier was undertaken to test the validity of available heavy-ion reaction theories. The nuclei  $^{54}\text{Fe}$  and  $^{62}\text{Ni}$  were chosen as targets because the final states accessible by the single proton transfers ( $^{16}\text{O}$ ,  $^{15}\text{N}$ ) and ( $^{12}\text{C}$ ,  $^{11}\text{B}$ ) include many different spins:  $1f_{7/2}$ ,  $1f_{5/2}$ ,  $2p_{3/2}$ ,  $2p_{1/2}$ , and  $1g_{9/2}$ . The  $^{16}\text{O}$  and  $^{12}\text{C}$  beam energies selected have the same energy per nucleon and hence similar kinematics.

Our initial analysis of the ( $^{16}\text{O}$ ,  $^{15}\text{N}$ ) and ( $^{12}\text{C}$ ,  $^{11}\text{B}$ ) reactions using the no-recoil distorted-wave Born approximation (DWBA) has been reported previously.<sup>1</sup> The  $j$  dependence predicted by the DWBA selection rules was confirmed, but the observed effect was a factor of  $\approx 3$  smaller than predicted. The failure of conventional DWBA has been ascribed to the no-recoil approximation<sup>2–5</sup> and it has been shown that inclusion of recoil introduces energy-dependent terms in the DWBA amplitudes.<sup>2–4</sup> Thus, study of ( $^{16}\text{O}$ ,  $^{15}\text{N}$ ) and ( $^{12}\text{C}$ ,  $^{11}\text{B}$ ) at 100 MeV ( $\approx 3$ – $4$  times Coulomb barrier) provides a stringent test of recoil effects.

In this paper we present analyses of  $^{54}\text{Fe}$ ,  $^{62}\text{Ni}$ -( $^{16}\text{O}$ ,  $^{15}\text{N}$ ) and  $^{54}\text{Fe}$ ,  $^{62}\text{Ni}$ ( $^{12}\text{C}$ ,  $^{11}\text{B}$ ) at energies:  $E(^{16}\text{O}) = 104$  MeV and  $E(^{12}\text{C}) = 78$  MeV using DWBA with and without recoil. The results are compared with those from ( $^3\text{He}$ ,  $d$ ), ( $\alpha$ ,  $t$ ) and low energy heavy-ion transfers. It is shown that DWBA with recoil yields consistent spectroscopic factors over a wide

range of bombarding energy and  $L$  transfers for the ( $^{16}\text{O}$ ,  $^{15}\text{N}$ ) and ( $^{12}\text{C}$ ,  $^{11}\text{B}$ ) reactions. Furthermore, the use of DWBA with recoil allows one to make  $j$  assignments for some levels.

## II. EXPERIMENTAL PROCEDURES

The experiments were performed with 78-MeV  $^{12}\text{C}^{3+}$  and 104-MeV  $^{16}\text{O}^{4+}$  beams from the Lawrence Berkeley Laboratory 88-inch cyclotron. The targets consisted of isotopically enriched  $^{54}\text{Fe}$  and  $^{62}\text{Ni}$  evaporated as layers 80–200  $\mu\text{g}/\text{cm}^2$  onto thin carbon backings. Reaction products were detected with a multiwire position-sensitive proportional counter in the focal plane of an energy-loss magnetic spectrometer.<sup>6</sup> The data were obtained event by event, stored on magnetic tape, and analyzed off-line. The relative integrated beam currents were deduced by means of a solid-state detector placed in the target chamber and target thicknesses were obtained from the elastic scattering at a forward angle where the scattering was mostly pure Rutherford. The energy resolution was typically 100–200 keV full width at half-maximum (FWHM).

## III. EXPERIMENTAL RESULTS

### A. Spectra

Spectra obtained near the grazing angles ( $\approx 15^\circ$  lab) are shown in Figs. 1 and 2. States of known spin and parity are indicated. In Tables I and II we list the groups observed in the present experi-

ment and compare these with levels observed in other experiments. Besides known states in  $^{55}\text{Co}$  and  $^{63}\text{Cu}$ , evidence for transfer to  $^{11}\text{B}^*(E_x \approx 2 \text{ MeV})$  and  $^{15}\text{N}^*(E_x \approx 7 \text{ MeV})$  is observed. The resulting groups (see Figs. 1 and 2) are broadened, presumably by  $\gamma$  decay in flight. Similar observations have been reported in the mass 90 region.<sup>7</sup>

Most of the transfer strength is observed in the region  $E_x = 0$  to 6 MeV. This is due partly to kinematics which favor  $Q \approx Q_{g.s.}$  for the targets  $^{54}\text{Fe}$  and  $^{62}\text{Ni}$ , and partly to the fragmentation of the single particle strength at high excitation.

As noted previously,<sup>1</sup> the  $(^{16}\text{O}, ^{15}\text{N})$  and  $(^{12}\text{C}, ^{11}\text{B})$  reactions favor different types of states, namely, the  $j_> (\equiv l + \frac{1}{2})$  final states are favored in  $(^{16}\text{O}, ^{15}\text{N})$  compared to  $(^{12}\text{C}, ^{11}\text{B})$  or light-ion reactions.

### B. Elastic scattering

The elastic scattering of  $^{12}\text{C}$  and  $^{16}\text{O}$  from  $^{54}\text{Fe}$  and  $^{62}\text{Ni}$  at  $E(^{12}\text{C}) = 78 \text{ MeV}$  and  $E(^{16}\text{O}) = 104 \text{ MeV}$  was obtained along with the transfer data. The angular distributions are shown in Fig. 3 as ratio to Rutherford scattering. The forward angle points have been normalized to Rutherford scattering and

the resulting data are believed to be accurate to  $\pm 8\%$ .

The elastic scattering resembles that obtained at lower bombarding energies<sup>8</sup> except that the grazing angle has moved forward to  $\approx 20^\circ$  c.m. The curves shown are optical model fits and are discussed in Sec. IV B.

### C. Transfer angular distributions

The angular distributions for groups observed in the transfer reactions (Figs. 1 and 2, Tables I and II) are shown in Figs. 4 and 5. These measurements were made with a  $0.6^\circ$  spectrometer aperture so the points represent cross sections averaged over this angular acceptance. Most of the angular distributions are of a similar shape: a monotonic increase up to the grazing angle ( $\theta \approx 20^\circ$ ), and inflection or maximum at the grazing angle and then a drop or slight rise at forward angles. There is some indication that the cross sections for low  $l$  transfers, i.e., low spin states are lower at forward angles compared to high spin states, e.g.,  $^{63}\text{Cu}$  g.s. ( $2p_{3/2}$ ) compared with  $^{63}\text{Cu}$ ,  $E_x = 2.49 \text{ MeV}$  ( $1g_{9/2}$ ). There

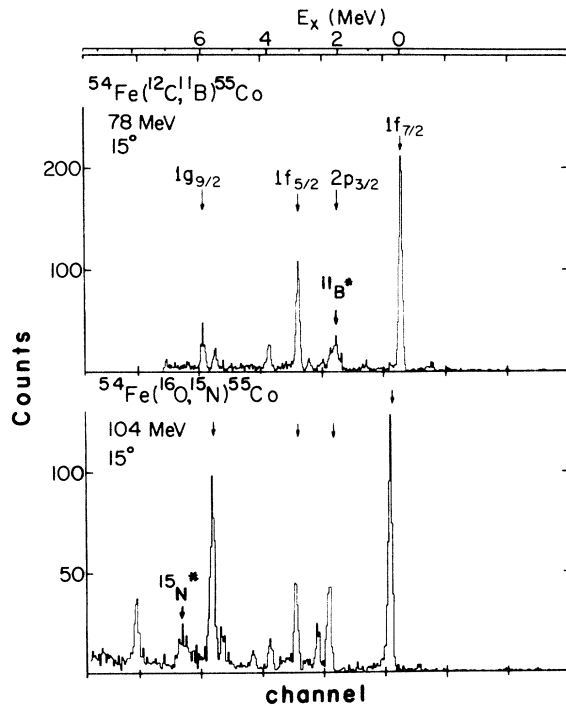


FIG. 1. Position ( $B\rho$ ) spectrum for  $^{54}\text{Fe}(^{12}\text{C}, ^{11}\text{B})^{55}\text{Co}$  and  $^{54}\text{Fe}(^{16}\text{O}, ^{15}\text{N})^{55}\text{Co}$ . The horizontal scales have been adjusted to give approximately the same energy per channel. Positions of single particle states in  $^{55}\text{Co}$ ,  $^{11}\text{B}$ , and  $^{15}\text{N}$  are indicated (see also Table I).

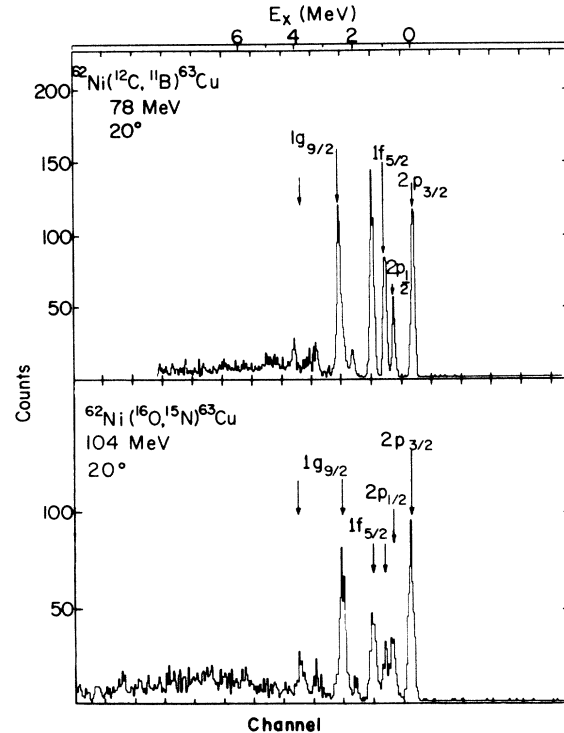


FIG. 2. Position ( $B\rho$ ) spectrum for  $^{62}\text{Ni}(^{12}\text{C}, ^{11}\text{B})^{63}\text{Cu}$  and  $^{62}\text{Ni}(^{16}\text{O}, ^{15}\text{N})^{63}\text{Cu}$ . The horizontal scales have been adjusted to give approximately the same energy per channel. Positions of known single particle states in  $^{63}\text{Cu}$  (see Table II) are indicated.

is also an effect of the  $Q$  value on the shapes which is not completely understood as yet (see Sec. IVD) and which could make  $l$  assignments based on angular distributions uncertain. The orbital angular momenta ( $l$ ) of most of the states observed in the present experiment are known from light-ion work,

however. The curves shown in Figs. 4 and 5 are DWBA calculations which include recoil. These are discussed in Sec. IVD.

It has been observed that angular distributions for some heavy-ion transfers, mostly two-nucleon transfers, exhibit rapid oscillations.<sup>9</sup> Our data

TABLE I. Levels observed in  $^{54}\text{Fe}(^{12}\text{C}, ^{11}\text{B})^{55}\text{Co}$  and  $^{54}\text{Fe}(^{16}\text{O}, ^{15}\text{N})^{55}\text{Co}$  compared with other experiments.

$E_x^b$ (MeV)	This work ( $^{12}\text{C}, ^{11}\text{B}$ ) $E=78$ MeV				$(^{16}\text{O}, ^{15}\text{N})$ $E=104$ MeV					Adopted $J^\pi$ g	Previous work <sup>a</sup> ( $^3\text{He}, d$ ) and ( $\alpha, t$ )			
	$\sigma_{\text{gr}}^c$ (mb/sr)	$L^d$	$J^\pi e$	$C^2S^f$	$E_x^b$ (MeV)	$\sigma_{\text{gr}}^c$ (mb/sr)	$L^d$	$J^\pi e$	$C^2S^f$		$E_x$ (MeV)	$l_p^h$	$J^\pi i$	$C^2S$
g.s.	2.72	<u>2, 3</u> , 4	$\frac{7}{2}^-$	0.25	g.s.	7.42	<u>3</u> , 4	$\frac{1}{2}^-$	0.35	$\frac{7}{2}^-$	g.s.	3	$\frac{7}{2}^-$	0.21–0.25
					2.13	2.88	<u>1</u> , 2	$\frac{3}{2}^-$	0.44	$\frac{3}{2}^-$	2.162	1	$\frac{3}{2}^-$	0.28–0.42
2.57	0.13	<u>0, 1</u> , 2	$\frac{1}{2}^-$	0.15	2.50	1.47	<u>0, 1</u>	$\frac{1}{2}^-$	1.51		2.559	1	( $\frac{1}{2}^-$ )	0.32–0.52
		<u>0, 1</u> , 2	$\frac{3}{2}^-$	0.13			<u>1</u> , 2	$\frac{3}{2}^-$	0.22	$\frac{3}{2}^-$			( $\frac{3}{2}^-$ )	0.21
2.95	0.16	<u>0, 1</u> , 2	$\frac{3}{2}^-$	0.17	2.90	0.55	<u>1</u> , 2	$\frac{3}{2}^-$	0.08		2.938 <sup>j</sup>	1	( $\frac{3}{2}^-$ )	0.28 <sup>j</sup>
		<u>0, 1</u> , 2	$\frac{1}{2}^-$	0.20			<u>0, 1</u>	$\frac{1}{2}^-$	0.56	$\frac{1}{2}^-$			( $\frac{1}{2}^-$ )	0.45 <sup>j</sup>
3.30	1.41				3.22	2.80					3.327 <sup>j</sup>	1	$\frac{3}{2}^-$	0.09–0.17
		<u>2, 3</u> , 4	$\frac{5}{2}^-$	0.92			<u>2, 3</u>	$\frac{5}{2}^-$	0.83	( $\frac{5}{2}^-$ )		+3	$\frac{5}{2}^-$	0.37–0.54
					3.65	0.80	<u>1</u> , 2	$\frac{3}{2}^-$	0.12	$\frac{3}{2}^-$	3.657	1	( $\frac{3}{2}^-$ )	0.07
							<u>0, 1</u>	$\frac{1}{2}^-$	0.82				( $\frac{1}{2}^-$ )	0.11
4.17	0.45				4.14	1.13					4.185 <sup>j</sup>	1	$\frac{1}{2}^-$	0.08–0.23 <sup>j</sup>
		<u>2, 3</u> , 4	$\frac{5}{2}^-$	0.38			<u>2, 3</u>	$\frac{5}{2}^-$	0.33	( $\frac{5}{2}^-$ )		+3	$\frac{5}{2}^-$	0.20–0.22 <sup>j</sup>
					4.70	0.78	<u>1</u> , 2	$\frac{3}{2}^-$	0.14	$\frac{3}{2}^-$	4.755 <sup>k</sup>	1	$\frac{3}{2}^-$	0.13–0.23
5.74	0.27	<u>2, 3</u> , 4	$\frac{5}{2}^-$	0.29	5.61	1.35	<u>2, 3</u>	$\frac{5}{2}^-$	0.42	( $\frac{5}{2}^-$ )	5.765 <sup>k</sup>	3	$\frac{5}{2}^-$	0.26–0.32
6.07	0.51	<u>3, 4</u> , 5	$\frac{9}{2}^+$	0.21	6.00	6.53	<u>4, 5</u>	$\frac{9}{2}^+$	0.40	$\frac{9}{2}^+$	6.080	4	$\frac{9}{2}^+$	0.16–0.50
					8.44	2.81	<u>4, 5</u>	$\frac{9}{2}^+$	0.19	( $\frac{9}{2}^+$ )	8.5 <sup>k</sup>	4	( $\frac{9}{2}^+$ )	
					8.96	0.50	<u>4, 5</u>	$\frac{9}{2}^+$	0.04					
2.0–2.4 <sup>l</sup>	2.70	<u>3</u> , 4	$\frac{7}{2}^-$	$\sim 0.4$ <sup>l</sup>	$\sim 7$ <sup>m</sup>	2.6								

<sup>a</sup> References 24–26. The excitation energies are taken from Ref. 25 and are said to be accurate to  $\pm 30$  keV. The range of spectroscopic factors listed have been deduced from the data compiled in Ref. 24, assuming the  $J^\pi$  value indicated. Only levels having  $C^2S \geq 0.1$  are listed.

<sup>b</sup> Excitation energy of target and/or projectile. Estimated error is  $\pm 50$  keV.

<sup>c</sup> Observed differential cross section (c.m.) near the grazing angle ( $\approx 15^\circ$  lab).

<sup>d</sup> The orbital angular momentum transfers permitted by Eq. (6). The nonnormal parity  $L$  transfers allowed with recoil are underlined.

<sup>e</sup> The spin and parity of the final target state assumed in the DWBA calculations.

<sup>f</sup> The spectroscopic factor for levels in  $^{55}\text{Co}$  as deduced from DWBA, with recoil, for the  $J^\pi$  value listed. The projectile spectroscopic factors ( $^{11}\text{B}$  g.s.:  $C^2S=2.98$  and  $^{15}\text{N}$  g.s.:  $C^2S=2.14$ ) are taken from Refs. 22 and 23, respectively, and the bound-state parameters are those used in Ref. 5. The fits to data for levels at large excitation energies are poor (see Fig. 4).

<sup>g</sup> The  $J^\pi$  value ( $^{55}\text{Co}$ ) which, we believe, yields the most consistent spectroscopic factors from analyses of the heavy-ion and light-ion data (see text). Uncertain values are bracketed.

<sup>h</sup> Orbital angular momentum of the transferred proton ( $=l$  of final state) from Ref. 25.

<sup>i</sup> Spin and parity of states in  $^{55}\text{Co}$  as deduced from light-ion experiments (Refs. 25 and 26). Bracketed values are uncertain.

<sup>j</sup> Probable doublet.

<sup>k</sup> Isobaric analog of  $^{55}\text{Fe}$  (Ref. 26).

<sup>l</sup> Believed to be due to transfer to excited state of  $^{11}\text{B}$ :  $E_x=2.14$  MeV,  $J^\pi=\frac{1}{2}^-$ ,  $C^2S=0.78$  (Ref. 22). See text.

<sup>m</sup> Believed to be due to transfer to excited states of  $^{15}\text{N}$ :  $E_x=6-7$  MeV (Ref. 23).

are not complete enough to establish if such oscillations are present in the angular distributions studied here. Most of our calculations (see Sec. IVD) do not exhibit appreciable oscillations, particularly near the grazing angle, although this may only be a consequence of using certain optical parameters, etc. As most of our results are determined by fitting data near the grazing angle, the presence of undetected oscillations at forward

or backward angles would not substantially affect the conclusions presented here.

#### IV. ANALYSIS

##### A. Semiclassical interpretation

Although the angular distribution ( $d\sigma/d\Omega$ ) observed at our bombarding energies do not appear to be the classical "bell" shape observed at lower

TABLE II. Levels observed in  $^{62}\text{Ni}(^{12}\text{C}, ^{11}\text{B})^{63}\text{Cu}$  and  $^{62}\text{Ni}(^{16}\text{O}, ^{15}\text{N})^{63}\text{Cu}$  compared with other experiments.

This work ( $^{12}\text{C}, ^{11}\text{B}$ ) $E=78$ MeV					$(^{16}\text{O}, ^{15}\text{N})$ $E=104$ MeV					Previous work <sup>a</sup> ( $^3\text{He}, d$ ) and ( $\alpha, t$ )				
$E_x^b$ (MeV)	$\sigma_{gr}^c$ (mb/sr)	$L^d$	$J^\pi e$	$C^2S^f$	$E_x^b$ (MeV)	$\sigma_{gr}^c$ (mb/sr)	$L^d$	$J^\pi e$	$C^2S^f$	Adopted $J^\pi g$	$E_x$ (MeV)	$l_p^h$	$J^\pi i$	$C^2S$
g.s.	2.31	<u>0, 1, 2</u>	$\frac{3}{2}^-$	0.40	g.s.	7.04	<u>1, 2</u>	$\frac{3}{2}^-$	0.50	$\frac{3}{2}^-$	g.s.	1	$\frac{3}{2}^-$	0.56–0.66
0.67	0.86	<u>0, 1, 2</u>	$\frac{1}{2}^-$	0.27	0.70	2.07	<u>0, 1</u>	$\frac{1}{2}^-$	0.57	$\frac{1}{2}^-$	0.67	1	$\frac{1}{2}^-$	0.70–0.76
		<u>0, 1, 2</u>	$\frac{3}{2}^-$	0.15			<u>1, 2</u>	$\frac{3}{2}^-$	0.21				$(\frac{3}{2}^-)$	0.35–0.38
0.97	1.89	<u>2, 3, 4</u>	$\frac{5}{2}^-$	0.19	0.96	2.38	<u>2, 3</u>	$\frac{5}{2}^-$	0.44	$\frac{5}{2}^-$	0.96	3	$\frac{5}{2}^-$	0.33–0.40
		<u>2, 3, 4</u>	$\frac{7}{2}^-$	0.17			<u>3, 4</u>	$\frac{7}{2}^-$	0.18				$(\frac{7}{2}^-)$	0.25–0.33
1.40	2.54	<u>2, 3, 4</u>	$\frac{5}{2}^-$	0.26	1.39	3.79	<u>2, 3</u>	$\frac{5}{2}^-$	0.45	$\frac{5}{2}^-$	1.41	3	$\frac{5}{2}^-$	0.45–0.68
		<u>2, 3, 4</u>	$\frac{7}{2}^-$	0.23			<u>3, 4</u>	$\frac{7}{2}^-$	0.18				$(\frac{7}{2}^-)$	0.38–0.51
					2.03	0.55	<u>0, 1</u>	$\frac{1}{2}^-$	0.30	$(\frac{1}{2}^-)$	2.06 <sup>j</sup>	1	$(\frac{1}{2}^-)$	0.23
							<u>1, 2</u>	$\frac{3}{2}^-$	0.08				$(\frac{3}{2}^-)$	0.12
2.52	2.64	<u>3, 4, 5</u>	$\frac{9}{2}^+$	0.22	2.49	6.89	<u>4, 5</u>	$\frac{9}{2}^+$	0.28	$\frac{9}{2}^+$	2.51	4	$(\frac{9}{2}^+)$	0.28–0.31
3.28	0.36	<u>2, 3, 4</u>	$\frac{5}{2}^-$	0.07	3.10	0.55	<u>2, 3</u>	$\frac{5}{2}^-$	0.10	$\frac{5}{2}^-$	3.23	3	$(\frac{5}{2}^-)$	0.06
3.50	0.55	<u>1, 2, 3</u>	$\frac{5}{2}^+$	0.04	3.46	1.01	<u>2, 3</u>	$\frac{5}{2}^+$	0.07	$\frac{5}{2}^+$	3.48	2	$(\frac{5}{2}^+)$	0.07
3.97	0.92	<u>3, 4, 5</u>	$\frac{9}{2}^+$	0.13	3.96	2.15	<u>4, 5</u>	$\frac{9}{2}^+$	0.08	$\frac{9}{2}^+$	3.98	4	$(\frac{9}{2}^+)$	0.05
					4.89	0.9	<u>4, 5</u>	$\frac{9}{2}^+$	0.03	$(\frac{9}{2}^+)$				
2.0–2.5 <sup>k</sup>	0.86	<u>1, 2</u>	$\frac{3}{2}^-$	$\sim 0.6^k$	7 <sup>l</sup>	8.0								
					9.81 <sup>l</sup>	1.07								

<sup>a</sup> References 27–29. The excitation energies are taken from Ref. 28 and are said to be accurate to  $\pm 50$  keV. The range of spectroscopic factors listed have been deduced from the data compiled in Ref. 27, assuming the  $J^\pi$  value indicated. Only levels having  $C^2S \geq 0.1$  are listed.

<sup>b</sup> Excitation energy of target and/or projectile. Estimated error is  $\pm 50$  keV.

<sup>c</sup> Observed differential cross section (c.m.) near the grazing angle ( $\approx 15^\circ$  lab).

<sup>d</sup> The orbital angular momentum transfers permitted by Eq. (6). The nonnormal parity  $L$  transfers allowed with recoil are underlined.

<sup>e</sup> The spin and parity of the final target state assumed in the DWBA calculation.

<sup>f</sup> The spectroscopic factor for levels in  $^{63}\text{Cu}$  as deduced from DWBA, with recoil, for the  $J^\pi$  value listed. The projectile spectroscopic factors ( $^{11}\text{B}$  g.s.:  $C^2S=2.98$  and  $^{15}\text{N}$  g.s.:  $C^2S=2.14$ ) are taken from Refs. 22 and 23, respectively, and the bound-state parameters are those used in Ref. 5. The fits to data for levels at large excitation energies are poor (see Fig. 5).

<sup>g</sup> The  $J^\pi$  value ( $^{63}\text{Cu}$ ) which, we believe, yields the most consistent spectroscopic factors from analyses of the heavy-ion and light-ion data (see text). Uncertain values are bracketed.

<sup>h</sup> Orbital angular momentum of the transferred proton ( $=l$  of final state) from Ref. 28.

<sup>i</sup> Spin and parity of states in  $^{63}\text{Cu}$  as deduced or assumed from light-ion experiments (Refs. 28 and 29). Bracketed values are uncertain.

<sup>j</sup> Probable doublet.

<sup>k</sup> Believed to be due to transfer to excited state of  $^{11}\text{B}$ :  $E_x=2.14$  MeV,  $J^\pi=\frac{1}{2}^-$ ,  $C^2S=0.78$  (Ref. 22). See text.

<sup>l</sup> Believed to be due to transfer to excited state of  $^{15}\text{N}$ :  $E_x=6-7$  MeV (Ref. 23). The 9.81 MeV level would correspond to excitation of both  $^{63}\text{Cu}$  ( $E_x \approx 2.5$  MeV) and  $^{15}\text{N}$ .

bombarding energies for these nuclei,<sup>10, 11</sup> this is somewhat deceiving in that one should remove the  $\theta$  dependence of  $d\Omega$ . In semiclassical theory this is done by plotting the apsidal distance distribution<sup>12</sup>  $d\sigma/dD$  defined by

$$\frac{d\sigma}{dD} = \frac{8\pi k}{\eta} \sin^3 \frac{1}{2}\theta \frac{d\sigma}{d\Omega}, \quad (1)$$

where  $k$  and  $\eta$  are the average wave number and Coulomb parameter and  $\theta$  is the c.m. scattering angle. The apsidal distance (assuming Rutherford orbits) is given by

$$D(\theta) = \frac{\eta}{k} (1 + \csc \frac{1}{2}\theta). \quad (2)$$

It is also useful to define a radius parameter  $d_0$  given by  $d_0 = D/(A_1^{1/3} + A_2^{1/3})$ , where  $A_1$  and  $A_2$  are the projectile and target mass numbers.

In Fig. 6 we show  $d\sigma/dD$  vs  $d_0$  as observed for  $^{54}\text{Fe}(^{16}\text{O}, ^{15}\text{N})^{55}\text{Co}$  (g.s.) at  $E_L = 104$  MeV and compare it with results obtained at 60 MeV.<sup>10</sup> The data obtained for other groups are similar. It is seen that  $d\sigma/dD$  is still "bell" shaped and peaked at  $d_0 \approx 1.9$  fm, i.e., well outside the nucleus. This value of  $d_0$  is to be compared to  $d_0 \approx 1.6-1.8$  fm obtained at lower energies.<sup>10, 11</sup> The apparent increase in  $d_0$  at higher bombarding energies can be

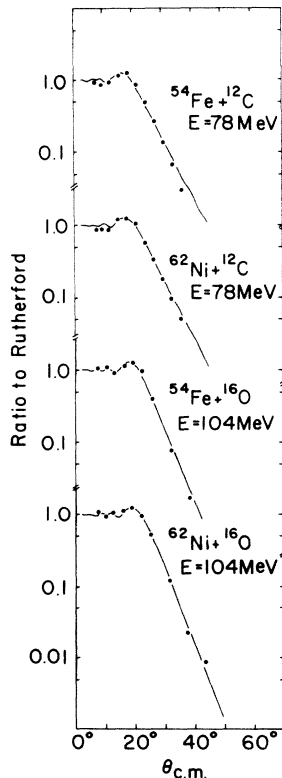


FIG. 3. Elastic scattering and optical model fits using parameters listed in Sec. IV B.

ascribed to distortions arising from the nuclear potential, and other effects.

As suggested in Ref. 10, we may remove most of the bell shape exhibited in  $d\sigma/dD$  by dividing out the effect of projectile absorption, using the measured elastic scattering  $\sigma_{el}(D)$ , to obtain a transfer probability,  $P_{tr}(D)$ , given by

$$P_{tr}(D) = (d\sigma/dD) \div \sigma_{el}(D). \quad (3)$$

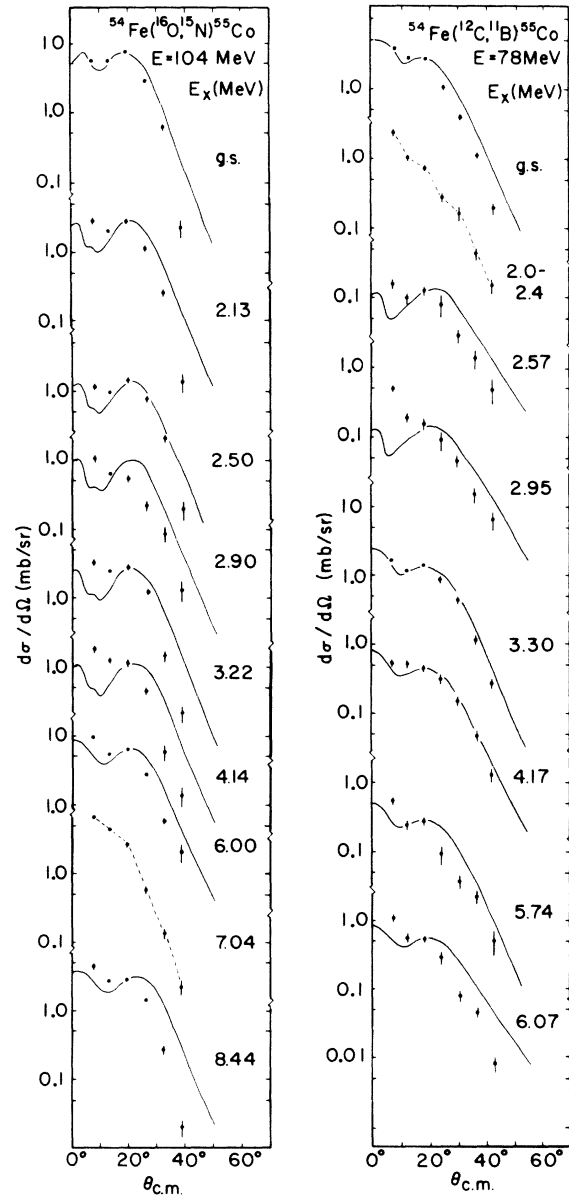


FIG. 4. Transfer data for  $^{54}\text{Fe}$  target. The solid curves are DWBA calculations with recoil. The excitation energies measured in the present experiment ( $\pm 50$  keV) are indicated. The dashed lines connect data points from groups believed to be the result of transfer to excited states of the outgoing projectile (see text).

One can parametrize  $P_{tr}(D)$ :

$$P_{tr}(D) \approx \mathcal{N} \exp[-KD(\theta)] \quad (4)$$

with  $K \approx 2\alpha$ , where  $\alpha$  is the decay constant of the wave function of the transferred nucleon averaged over the projectile and target, and  $\mathcal{N}$  is approximately constant. Usually,  $K$  must be adjusted slightly to fit the angular distribution well.

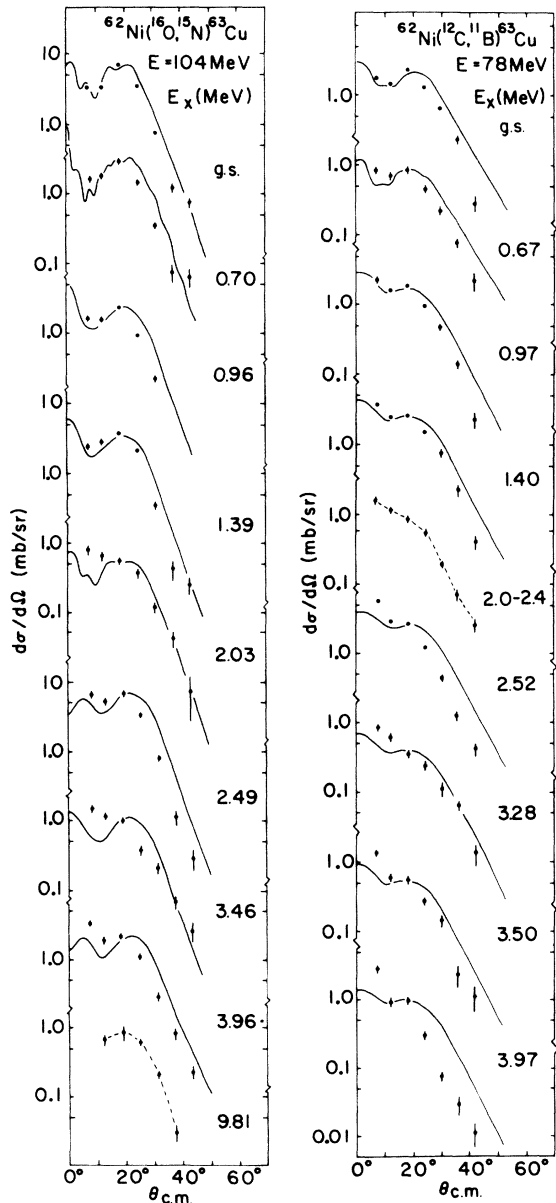


FIG. 5. Transfer data for  $^{62}\text{Ni}$  target. The solid curves are DWBA calculations with recoil. The excitation energies measured in the present experiment ( $\pm 50$  keV) are indicated. The dashed lines connect data points from groups believed to be the result of transfer to excited states of the outgoing projectile (see text).

Using Eqs. (3) and (4), we obtain  $K \approx 0.44 \text{ fm}^{-1}$  for the 104-MeV  $(^{16}\text{O}, ^{15}\text{N})$  data shown in Fig. 6. This is to be compared to  $K \approx 0.68 \text{ fm}^{-1}$  obtained at 60 MeV<sup>10</sup> and the theoretical value  $K \approx 2\alpha = 0.72 \text{ fm}^{-1}$  expected at sub-Coulomb energies. The decrease of  $K$  with bombarding energy is not unexpected as  $K \approx 2\alpha$  only if the transfer takes place at the orbit turning point.<sup>12</sup> This is probably a poor approximation at high energies, although qualitatively Eqs. (3) and (4) exhibit the correct features even at these energies and are therefore useful concepts.

### B. Optical model analysis

The elastic scattering (Fig. 3) has been fitted using the optical model with Woods-Saxon potentials having a volume form factor. Reasonable fits were obtained with the parameters<sup>8</sup>  $R = 1.30 (A_1^{1/3} + A_2^{1/3}) \text{ fm}$ ,  $a = 0.5 \text{ fm}$ , and adjusting  $V$  and  $W$ . The results shown in Fig. 3 have  $V = -25 \text{ MeV}$  and  $W = -15 \text{ MeV}$  which is to be compared with  $V \approx -40 \text{ MeV}$  and  $W = -15 \text{ MeV}$  found<sup>8</sup> at 60 MeV.

### C. DWBA without recoil

We have performed no-recoil DWBA calculations<sup>13</sup> with finite range form factors.<sup>14</sup> The no-

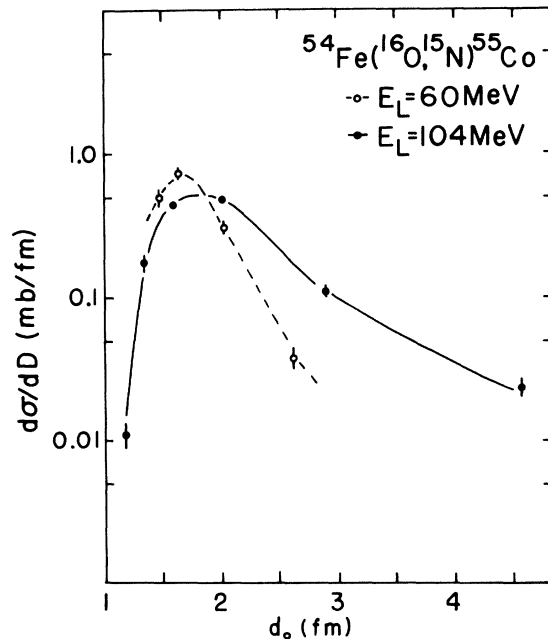


FIG. 6. The apsidal distributions for  $^{54}\text{Fe}(^{16}\text{O}, ^{15}\text{N})^{55}\text{Co}$  g.s. as deduced [Eqs. (1) and (2)] from measurements at bombarding energies of 60 MeV (Ref. 10) and 104 MeV (this experiment). The quantity  $d_0$  is the classical apsidal distance [Eq. (2)] divided by  $(A_1^{1/3} + A_2^{1/3})$ .

recoil selection rules are<sup>15</sup>

$$\begin{aligned} (^{16}\text{O}, ^{15}\text{N}): L = l+1 \text{ for } j=j_>, \\ L = l-1 \text{ for } j=j_<, \end{aligned} \quad (5)$$

$$(^{12}\text{C}, ^{11}\text{B}): L = l-1 \text{ and } l+1, j=j_> \text{ or } j_< ,$$

where  $L$  is the allowed angular momentum transfer and  $l$  and  $j$  are the orbital and total angular momenta of the transferred nucleon in the target (post-representation). In Eq. (5)  $j_> \equiv l + \frac{1}{2}$  and  $j_< \equiv l - \frac{1}{2}$ .

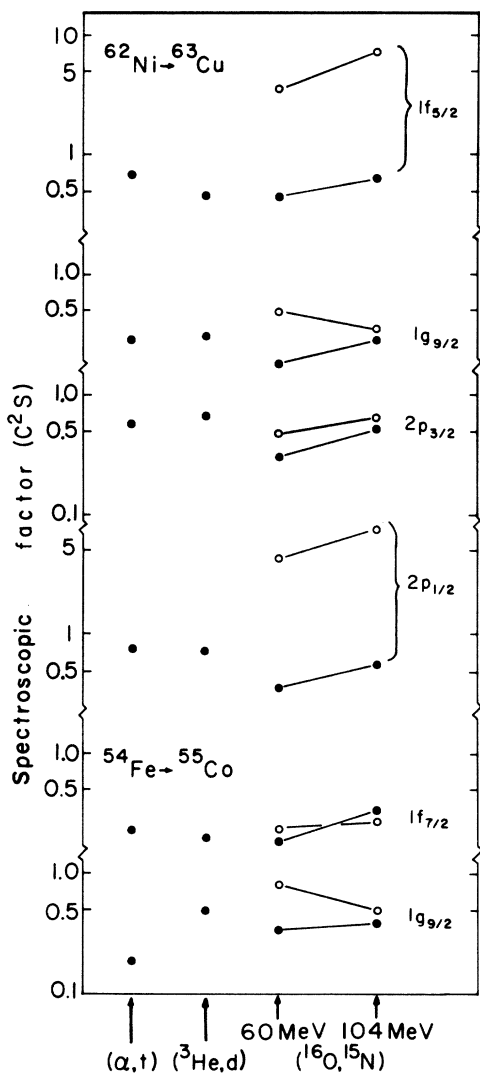


FIG. 7. A comparison of spectroscopic factors as deduced from light-ion (Refs. 24, 25, 28, and 29) and heavy-ion transfer reactions for the states indicated (see Tables I and II). The heavy-ion results are at bombarding energies of 60 MeV (Ref. 10) and 104 MeV (this experiment). The closed and open circles represent DWBA calculations with and without recoil, respectively.

The target spectroscopic factors ( $C^2S$ ) obtained with  $(^{16}\text{O}, ^{15}\text{N})$  for selected states in  $^{55}\text{Co}$  and  $^{63}\text{Cu}$  are shown in Fig. 7. We include also light-ion results and  $(^{16}\text{O}, ^{15}\text{N})$  results<sup>10</sup> at  $E = 60$  MeV. The no-recoil DWBA calculations employ a normalization factor obtained<sup>5</sup> from an analysis of  $^{208}\text{Pb}$ - $(^{16}\text{O}, ^{15}\text{N})$ .

As noted previously,<sup>5, 10, 11</sup> the target spectroscopic factors deduced for  $j_>$  states are reasonably consistent with light-ion results ( $C^2S \lesssim 1$ ), while those deduced for  $j_<$  states are grossly overestimated,<sup>5, 10</sup> e.g., by factors of 2 to 10. The discrepancies become more pronounced at high bombarding energies: at 60 MeV the apparent  $C^2S$  for  $^{63}\text{Cu}$   $j_<$  states ( $1f_{5/2}$  and  $2p_{3/2}$ ) are  $\approx 3$  to 4 while at 104 MeV one obtains  $C^2S \approx 7$ . The  $C^2S$  deduced for some  $j_>$  states also show large variations with bombarding energy. This suggests that no-recoil DWBA is probably unreliable for both  $j_>$  and  $j_<$  final states.

#### D. DWBA with recoil

Calculations have also been performed with the full finite-range DWBA program LOLA.<sup>16</sup> The inclusion of recoil introduces the so-called nonnormal parity  $L$  transfers: The selection rules are then<sup>2-5</sup>

$$\begin{aligned} (^{16}\text{O}, ^{15}\text{N}): L = l+1 \text{ and } l \text{ for } j=j_>, \\ L = l-1 \text{ and } l \text{ for } j=j_<, \end{aligned} \quad (6)$$

$$(^{12}\text{C}, ^{11}\text{B}): L = l-1, l, \text{ and } l+1, j=j_> \text{ or } j_< .$$

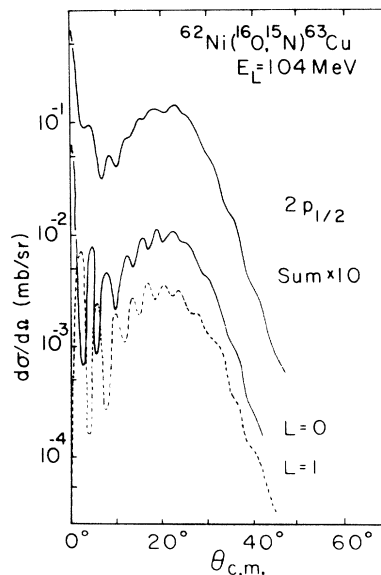


FIG. 8. A comparison of DWBA calculations (with recoil) for  $(^{16}\text{O}, ^{15}\text{N})$  to a  $j^\pi = 2p_{1/2}$  state. The normal parity ( $L=0$ , lower solid line) and nonnormal parity ( $L=1$ , dashed line) are shown separately and summed.

In all cases, then, the cross section will be an incoherent sum over several  $L$  transfers, with the largest  $L$  transfer usually favored kinematically. This latter feature affects the  $j_{<}$  states most strongly.<sup>5</sup> The normal and nonnormal parity  $L$  transfers allowed by (6) are listed in Tables I and II.

We illustrate the contributions of the normal and nonnormal  $L$  transfers in Fig. 8 for  $^{62}\text{Ni}(^{16}\text{O}, ^{15}\text{N})-^{63}\text{Cu } 2p_{1/2}$ . It should be noted that the contribution from the nonnormal  $L$  transfer vanishes, exactly, at  $\theta=0^\circ$  (and also  $180^\circ$ ), and that the angular distributions of the normal and nonnormal  $L$  transfers are out of phase, thus minimizing oscillations in the summed cross section. The relative contribution of the nonnormal  $L$  transfers to the cross sections at  $\theta \approx 20^\circ$  are as follows:  $(^{16}\text{O}, ^{15}\text{N})$ ,  $\sigma_{\text{nonnormal } L}/\sigma_{\text{normal } L} \approx 10\text{--}35\%$  while for  $(^{12}\text{C}, ^{11}\text{B})$ ,  $\sigma_{\text{nonnormal } L}/\sigma_{\text{normal } L} \approx 15\%$ . More important, however, is the effect of recoil on the DWBA amplitudes for all  $L$  transfers.<sup>3</sup>

In Figs. 4 and 5 we display the calculated angular distributions. The target spectroscopic factors deduced are given in Tables I and II and compared with light-ion results in the tables and in Fig. 7. We have also reanalyzed the  $(^{16}\text{O}, ^{15}\text{N})$  data at 60 MeV using DWBA with recoil, and these results are also shown in Fig. 7. The  $C^2S$  values deduced from the calculations including recoil assumed unity normalization and no parameters have been adjusted. It can be seen that the  $C^2S$  values obtained for both  $j_{>}$  and  $j_{<}$  states are now comparable to those obtained with light ions, and no longer display such dramatic variations with bombarding energy. There still are some discrepancies, e.g., the  $2p_{1/2}$  and  $2p_{3/2}$  cross sections are overestimated (if one assumes the light-ion results to be correct) compared with higher spin states. This most likely reflects inadequacies in the bound state potentials used, particularly the spin orbit potential, in that the different reactions are sensitive to different radial parts of the nuclear wave functions and not just the over-all normalization or spectroscopic factor.

The calculated angular distributions (Figs. 4 and 5) give acceptable fits (without parameter adjustments) to the data for transitions to levels near the g.s. in  $^{55}\text{Co}$  and  $^{63}\text{Cu}$ . These transitions have  $Q$  values yielding reasonably good momentum matching in the incident and outgoing channels, i.e.,  $Q \approx Q_{\text{opt}}$ .<sup>17, 18</sup> The more endothermic transitions are not fitted very well: the DWBA predictions (with or without recoil) shift back with increasingly negative  $Q$  value whereas the data do not and, if anything, they perhaps shift forward. This effect has been observed in many heavy-ion reactions<sup>5, 10, 11, 19</sup> and is not yet understood.

Calculations for groups involving projectile excitation, e.g.  $(^{12}\text{C}, ^{11}\text{B}^*) E_x = 2.0$  to  $2.4$  MeV, are not included in Figs. 4 and 5 as the measured cross sections rise much more rapidly at forward angles than predicted. This effect has been observed in other heavy-ion reactions.<sup>20</sup> In Tables I and II we have used peak or integrated cross sections to deduce spectroscopic factors where the DWBA fits are poor.

#### E. $j$ assignments

Unlike  $(^3\text{He}, d)$ ,  $(\alpha, t)$ , etc., the  $L$  transfer allowed in heavy-ion reactions such as  $(^{16}\text{O}, ^{15}\text{N})$  and  $(^{12}\text{C}, ^{11}\text{B})$  depends on the  $j$  value of the target state [see Eq. (6)]. Depending on the kinematics, i.e.,  $Q$  value for a given transition, the  $(^{16}\text{O}, ^{15}\text{N})$  and  $(^{12}\text{C}, ^{11}\text{B})$  cross sections for levels of the same  $l$  but different  $j$  may differ substantially. In principle, then, only the correct  $j$  value will give consistent spectroscopic factors between heavy-ion and light-ion data. Previous attempts to use this feature have been hampered by lack of reliable theoretical calculations.<sup>7</sup> Also, for some reactions, notably  $(^7\text{Li}, ^6\text{He})$ , the shapes of the angular distributions exhibit a  $j$  dependence.<sup>21</sup>

There are many levels in  $^{55}\text{Co}$  and  $^{63}\text{Cu}$  for which  $l$  values have been assigned. The  $j$  assignments, however, are less certain and often in conflict between different analyses. We have deduced spectroscopic factors for many such levels assuming both  $j = l + \frac{1}{2}$  and  $j = l - \frac{1}{2}$ . The results are listed in Tables I and II together with  $C^2S$  values for states where previous  $j$  assignments are thought to be reliable. A comparison of the  $(^{12}\text{C}, ^{11}\text{B})$ ,  $(^{16}\text{O}, ^{15}\text{N})$ , and the light-ion results permits a  $j$  assignment to be made or allows one to verify a previous assignment.

#### 1. Levels in $^{55}\text{Co}$

Based on the results given in Table I, the following information concerning the levels in  $^{55}\text{Co}$  is obtained: The 2.13, 2.57, 3.65, and 4.70 MeV states indicate  $j^\pi = \frac{3}{2}^-$ , while for  $E_x = 2.95$  MeV,  $j^\pi = \frac{1}{2}^-$  is preferred. The results for the levels at  $E_x = 3.30$ , 4.17, and 5.74 MeV are not inconsistent with the assignment  $j^\pi = \frac{5}{2}^-$ , although our  $C^2S$  values appear to be somewhat too large ( $\sum C^2S > 1$ ). The levels at  $E_x = 6$  and 8.5 MeV are seen as prominent groups in both  $(^{16}\text{O}, ^{15}\text{N})$  and  $(\alpha, t)$  and are likely  $j^\pi = \frac{9}{2}^+$  with  $C^2S \approx 0.4$  and  $0.2$ , respectively. Furthermore, we observe a level at  $E_x = 8.96$  MeV which would have  $C^2S = 0.04$  if  $j^\pi = \frac{9}{2}^+$ . No  $l$  assignments for this state are available, however.

#### 2. Levels in $^{63}\text{Cu}$

The situation for  $^{63}\text{Cu}$  is less favorable compared with  $^{55}\text{Co}$  regarding  $j$  assignments. Unlike



$^{55}\text{Co}$ , the  $Q$  values are such that kinematics apparently do not favor the larger  $L$  transfers. Thus, the spectroscopic factors deduced for some states are not distinct enough to permit unambiguous spin assignments. Some preferences are indicated, however.

The results for  $E_x = 0.70$  MeV appear most consistent for  $j^\pi = \frac{1}{2}^-$  (see Table II), since for  $j^\pi = \frac{3}{2}^-$  our  $C^2S$  values would then be  $\approx \frac{1}{2}$  the light-ion results. Similarly,  $j^\pi = \frac{5}{2}^-$  for  $E_x = 0.97$  and  $1.40$  MeV appears preferable to  $j^\pi = \frac{7}{2}^-$ , but the latter cannot be ruled out by our analysis. [In comparing our ( $^{12}\text{C}$ ,  $^{11}\text{B}$ ) and ( $^{16}\text{O}$ ,  $^{15}\text{N}$ ) spectroscopic factors, it should be noted that the former are consistently smaller than the latter. This, however, may reflect upon our choice for the projectile spectroscopic factors, etc.]

The ( $^{12}\text{C}$ ,  $^{11}\text{B}$ ) data for  $E_x = 2.0$  MeV were obscured by excitation of  $^{11}\text{B}$ , and thus only the ( $^{16}\text{O}$ ,  $^{15}\text{N}$ ) and light-ion data are available. These show a slight preference for  $j^\pi = \frac{1}{2}^-$ . The other groups, at  $E_x = 2.5$ ,  $3.2$ ,  $3.5$ , and  $4$  MeV indicate  $j^\pi = \frac{9}{2}^+$ ,  $\frac{5}{2}^-$ ,  $\frac{5}{2}^+$ , and  $\frac{9}{2}^+$ , respectively. The  $4.89$  MeV group seen in ( $^{16}\text{O}$ ,  $^{15}\text{N}$ ) is probably  $j^\pi = \frac{9}{2}^+$  ( $C^2S = 0.03$ ) as the  $Q$  value for this level is highly restrictive and favors high-spin states only.

#### F. Projectile excitation

The data for ( $^{12}\text{C}$ ,  $^{11}\text{B}^*$ ,  $E_x = 2$  MeV) have been used to deduce  $^{55}\text{Co}$  g.s. and  $^{63}\text{Cu}$  g.s. spectro-

scopic factors with  $^{11}\text{B}^* C^2S (= 0.8)$  taken from the literature<sup>22</sup> (see Table I and II). Alternately, we can use the ( $^{12}\text{C}$ ,  $^{11}\text{B}$ ) and ( $^{12}\text{C}$ ,  $^{11}\text{B}^*$ ) data to the same final states to deduce the spectroscopic factor for  $^{11}\text{B}^*$ . This gives

$$C^2S(^{11}\text{B}^*, E_x = 2 \text{ MeV}) = 1.14.$$

#### V. CONCLUSIONS

We conclude the following from the analysis of the ( $^{12}\text{C}$ ,  $^{11}\text{B}$ ) and ( $^{16}\text{O}$ ,  $^{15}\text{N}$ ) reactions on  $^{54}\text{Fe}$  and  $^{62}\text{Ni}$  at  $E(^{12}\text{C}) = 78$  and  $E(^{16}\text{O}) = 104$  MeV: (a) Full finite range DWBA, i.e., including recoil, gives adequate results whereas DWBA without recoil does not. (b) Certain features, such as the shift in grazing angle with  $Q$  value, however, are not reproduced by DWBA with or without recoil. (c) Analysis using full finite-range DWBA allows  $j$  assignments for certain levels, depending on the kinematic features of the transition.

#### ACKNOWLEDGMENTS

We thank C. Maguire, D. Miller, F. Pühlhofer, and J. Sherman for their assistance. We also thank the Lawrence Berkeley Laboratory cyclotron staff and crew for providing the necessary equipment and heavy-ion beams for this experiment.

<sup>†</sup>Work supported in part by the U. S. Atomic Energy Commission Contracts Nos. AEC AT(11-1)-2167 and W-7405-ENG-48.

\*Present address: Physics Division, Argonne National Laboratory, Argonne, Illinois 60439.

‡Present address: Physics Department, University of Washington, Seattle, Washington 98195.

<sup>1</sup>D. G. Kovar, F. D. Becchetti, B. G. Harvey, F. G. Pühlhofer, J. Mahoney, D. W. Miller, and M. S. Zisman, Phys. Rev. Lett. **29**, 1023 (1972).

<sup>2</sup>K. R. Greider, in *Nuclear Reactions Induced by Heavy Ions*, edited by R. Bock and W. Hering (North-Holland, Amsterdam, 1970).

<sup>3</sup>R. M. DeVries and K. I. Kubo, Phys. Rev. Lett. **30**, 325 (1973); L. A. Charlton, *ibid.* **31**, 116 (1973).

<sup>4</sup>M. A. Nagarajan, Nucl. Phys. **A196**, 34 (1972).

<sup>5</sup>D. G. Kovar, B. G. Harvey, F. D. Becchetti, J. Mahoney, D. L. Hendrie, H. Homeyer, W. von Oertzen, and M. A. Nagarajan, Phys. Rev. Lett. **30**, 1075 (1973).

<sup>6</sup>B. G. Harvey, J. Mahoney, F. G. Pühlhofer, F. S. Goulding, D. A. Landis, J.-C. Faivre, D. G. Kovar, M. S. Zisman, J. R. Meriwether, S. W. Cospser, and D. L. Hendrie, Nucl. Instrum. Methods **104**, 21 (1972).

<sup>7</sup>M. S. Zisman, F. D. Becchetti, B. G. Harvey, D. G. Kovar, J. Mahoney, and J. D. Sherman, Phys. Rev. **C 8**, 1866 (1973).

<sup>8</sup>F. D. Becchetti, P. R. Christensen, V. I. Manko, and

R. J. Nickles, Nucl. Phys. **A203**, 1 (1973).

<sup>9</sup>M. Schneider *et al.*, Phys. Rev. Lett. **31**, 320 (1973); C. Chasman *et al.*, *ibid.* **31**, 1074 (1973).

<sup>10</sup>P. R. Christensen, V. I. Manko, F. D. Becchetti, and R. J. Nickles, Nucl. Phys. **A207**, 33 (1973).

<sup>11</sup>H. J. Körner, G. C. Morrison, L. R. Greenwood, and R. H. Siemssen, Phys. Rev. **C 7**, 107 (1973).

<sup>12</sup>G. Breit and M. E. Ebel, Phys. Rev. **103**, 679 (1956).

<sup>13</sup>Program DWUCK, P. D. Kunz (unpublished).

<sup>14</sup>Program RDRC, W. Tobocman (unpublished).

<sup>15</sup>P. J. A. Buttle and L. J. B. Goldfarb, Nucl. Phys. **78**, 409 (1966).

<sup>16</sup>Program LOLA, R. DeVries (unpublished).

<sup>17</sup>P. J. A. Buttle and L. J. B. Goldfarb, Nucl. Phys. **A176**, 299 (1971).

<sup>18</sup>D. M. Brink, Phys. Lett. **40B**, 37 (1972).

<sup>19</sup>J. S. Larsen, J. L. C. Ford, Jr., R. M. Gaedke, K. S. Toth, J. B. Ball, and R. L. Hahn, Phys. Lett. **42B**, 205 (1972); J. V. Maher, K. A. Erb, and R. W. Miller, Phys. Rev. **C 7**, 651 (1973).

<sup>20</sup>R. H. Siemssen, C. L. Fink, L. R. Greenwood, and H. J. Körner, Phys. Rev. Lett. **28**, 626 (1972).

<sup>21</sup>R. L. White, K. W. Kemper, L. A. Charlton, and G. D. Gunn, Phys. Rev. Lett. **32**, 892 (1974).

<sup>22</sup>F. Hinterberger, G. Mairle, U. Schmidt-Rohr, P. Turek, and G. J. Wagner, Nucl. Phys. **A106**, 161 (1968).

- <sup>23</sup>J. C. Hiebert, E. Newman, and R. H. Bassel, *Phys. Rev.* 154, 898 (1967).
- <sup>24</sup>Nucl. Data B3 (Nos. 3, 4) (1970), edited by R. L. Auble and J. Rapaport.
- <sup>25</sup>B. Rosner and C. H. Holbrow, *Phys. Rev.* 154, 1080 (1967); G. Vourvopoulos, J. D. Fox, and B. Rosner, *ibid.* 177, 1789 (1969).
- <sup>26</sup>P. Roussel, G. Bruge, A. Bussiere, H. Faraggi, and J. E. Testoni, *Nucl. Phys.* A155, 306 (1970).
- <sup>27</sup>Nucl. Data B2(No. 3) (1967), edited by H. Verheul.
- <sup>28</sup>A. G. Blair, *Phys. Rev.* 140, B648 (1965).
- <sup>29</sup>D. D. Armstrong, A. G. Blair, and H. C. Thomas, *Phys. Rev.* 155, 1254 (1967).